

A.D. 1835 Eruption of Volcán Cosigüina, Nicaragua: A Guide for Assessing Hazards

By William Scott¹, Cynthia Gardner¹, Antonio Alvarez², and Graziella Devoli³

¹ Cascades Volcano Observatory, U.S. Geological Survey, 1300 SE Cardinal Court, Vancouver, WA 98683

² Instituto Nicaragüense de Estudios Territoriales (INETER), Código Postal 2110, Managua, Nicaragua

³ Norge Geotekniske Institutt, Sognsveien 72, P.B. 3930, Ullevaal Stadion, N-0806 Oslo, Norway

Intended for GSA Special Paper on Central American volcano hazards

Revised draft of 30 MAR 2005 following review by JD-N

ABSTRACT

The January 1835 eruption of Volcán Cosigüina in northwestern Nicaragua was one of the largest and most explosive in Central America since the Spanish Conquest. We report on the results of two weeks of reconnaissance stratigraphic studies and limited laboratory work aimed at better defining the distribution and character of deposits emplaced by the eruption as a means of developing a preliminary hazards assessment for future eruptions. On the lower flanks of the volcano, a basal tephra-fall deposit is composed of either ash and fine lithic lapilli or, locally, dacitic pumice. An overlying tephra-fall deposit forms an extensive blanket of brown to gray andesitic scoria that is 35 to 60 cm thick at 5 to 10 km from the summit-caldera rim except southwest of the volcano, where it is considerably thinner. The scoria fall produced the most voluminous deposit of the eruption and is overlain by pyroclastic-surge and -flow deposits that are composed chiefly of gray andesitic scoria. These flowage deposits form broad fans and valley fills in northern and southeastern sectors of the volcano that locally reach the Gulf

of Fonseca. An arcuate ridge that lies 2 km west of the caldera rim and a low ridge east of the caldera deflected most of the pyroclastic flows northward and southeastward. Pyroclastic flows did not reach the lower west and southwest flanks, which instead receive thick, fine-grained, accretionary-lapilli-rich ashfall deposits that probably were chiefly derived from ash clouds elutriated from pyroclastic flows. Following the eruption, large portions of the lower flanks were affected by lahars and rapid alluviation triggered by erosion of deposits and creation of new channels. Pre-1835 eruptions are poorly dated; however, scoria-fall, pyroclastic-flow, and lahar deposits record an eruption of probable lesser magnitude than that of 1835 a few centuries earlier—perhaps in the 15th century. An undated sequence of several thick tephra-fall deposits on the west flank of the volcano provides evidence of eruptions of probably greater magnitude than that of 1835. On the basis of weathering evidence, this sequence appears to be at least several thousand years old. The wide extent of pyroclastic flows and thick tephra fall during 1835, the greater magnitude of some previous Holocene eruptions, and the location of Cosigüina on a peninsula limit the options to reduce risk during future unrest and eruption.

INTRODUCTION

Nicaragua's largest and most explosive eruption in historical time climaxed 20-24 January 1835 at Volcán Cosigüina, which is located on a peninsula that forms the northwestern tip of the country (Fig. 1). Limited investigations on the north and east flanks of the volcano by Williams (1952) and Self and others (1989) provide a convincing case that the bulk volume of pyroclastic material produced ($<10 \text{ km}^3$) was

much smaller than most estimates (up to 150 km³) made by visitors in the years and decades following the eruption. During 2002 and 2003 we conducted about two weeks of field studies that included visits to the other flanks of the volcano. Here we describe the stratigraphy and distribution of 1835 pyroclastic-fall and -flow deposits and discuss their implications for eruption character and volume, provide geochemical data for eruptive products, comment briefly on evidence of pre-1835 eruptions at the volcano, and present a preliminary hazard assessment based on the 1835 event.

Williams (1952) and Self and others (1989) summarize the historical accounts of the eruption, which was noted for its wide dispersal of ash and great distance at which explosions were heard. Ashfall was reported northwestward to Chiapas, Mexico (600 km), southeastward to Costa Rica (350 km) and perhaps as far as Bogotá, Colombia (1900 km), and northeastward to Jamaica (1300 km). Booming sounds made soldiers in Guatemala and Belize think that they were under artillery attack, and noises were also heard in Oaxaca (Mexico), Jamaica, and Bogotá (Galindo, 1835a, b).

Cosigüina is a broad composite cone with a 2.5-km-wide summit caldera that contains a large lake. The highest point on the caldera rim is 872 m above sea level; the surface of the lake is at an altitude of about 160 m. A 200-to-300-m-high arcuate ridge lies on the west flank about 2 km outside the caldera rim. A broad ridge of andesitic lava flows, which we call Loma San Juan for one of its high points, forms the lower east-southeast sector of the volcano. These features deflected flows onto the north and south flanks, which merge into broad fans of pyroclastic-flow deposits, lahars, and alluvium.

Our observations build on the interpretations and three-fold succession of tephra deposits of the 1835 eruption presented by Self and others (1989) from sites on the eastern flank (Fig. 2, section A). Basal ash-rich beds (Set 1) were deposited by fall and surge processes thought to be associated with phreatic and phreatomagmatic eruptions. An overlying coarse-grained andesitic (58 to 60 wt. % SiO₂) scoria-fall deposit (Set 2) represents the major magmatic deposit of the eruption, thought to be vulcanian or plinian in nature. Pyroclastic-flow, -surge, and -fall deposits (Set 3) associated with vulcanian explosions bury the scoria-fall deposit and form fans on the lower flanks.

[Figure 1 near here]

STRATIGRAPHY OF 1835 DEPOSITS

We studied numerous sites on all flanks of the volcano (Figs. 1, 2) and found that the deposits of the 1835 eruption fit, in large part, Self and other's (1989) three-fold succession, but with some additional complexity. A prominent scoria-fall deposit is the most conspicuous, continuous, and easily traceable of the units attributed to the 1835 eruption, so we organize the following discussion about deposits in relation to their stratigraphic position with respect to the scoria fall.

[Figure 2 near here]

Deposits below scoria fall

Self and others (1989) designate as Set 1 a sequence of fall and surge deposits that underlies the scoria-fall deposit high on the east flank (Fig. 2; section A). In that proximal area, the lower part of Set 1 consists of thin fine-grained ash-fall and interbedded lithic lapilli-fall deposits. The upper part contains lithic-rich surge deposits with scoriaceous lenses. They interpret these deposits as originating from initial phreatic and phreatomagmatic explosions, in which the content of juvenile components increased with time.

In more distal sites, a few centimeters or less of fine-grained fall deposit composed of laminated, light-gray to brownish-gray ash and fine lapilli underlie the scoria-fall deposit (Fig. 2, sections B-F). Its color, texture, and position with respect to the scoria-fall deposit are consistent with correlation to Set 1 of Self and others (1989). Most of the sand-sized ash and fine lapilli are composed of angular to subrounded grains of poorly to moderately vesicular, gray to black, glassy andesite. Free crystals of plagioclase, hypersthene, and augite are also present, as is rare white to light-gray pumice. Typically a few percent of grains are variably hydrothermally altered and likely accidental fragments. Our observations suggest that these deposits contain substantially more juvenile material (>75%) than Self and others (1989) reported in the proximal deposits (<5%). Between sections F and G on the southwest flank, the basal ash thickens gradually from 2 to 50 cm. As it does so, the upper part coarsens and develops a definable subunit

of laminated, gray to pinkish-gray, medium to coarse ash and fine lithic lapilli (see Figure 9). In section H, which lies on the shoulder of a broad ridge on the west flank, this unit is composed of 40 cm of friable, well-bedded (thin-planar beds to low-angle cross beds) medium and coarse ash with beds and lenses of subangular to subrounded fine lithic lapilli. The deposit has some characteristics of a surge deposit, but because we don't see similar sediments elsewhere, we suspect that it is probably a fall deposit that was partly reworked during its accumulation on a slope to form the cross beds. On the basis of the distribution (Fig. 3A) and texture of this lower unit, we infer that the tephra was dispersed chiefly by prevailing low-altitude northeasterly to easterly winds and therefore associated with relatively low (<6 km) eruption columns.

[Figure 3 near here]

[Table 1 near here]

A conspicuous layer of white to light-gray dacitic (65 wt.% SiO₂; Table 1, samples 16 and 17; Fig. 4) pumice, the most silicic product of the 1835 eruption, is present in pre-scoria-fall deposits in many exposures on the lower flanks, except in southeast to southwest sectors (Figs. 2, 3B). The location of the thickest and coarsest units of this pumice implies dispersal by southerly winds. Its stratigraphic position varies in relation to the basal fine ashfall deposit. In some areas a scattering (section B) to as much as 18 cm (sections H, K, and L) of pumice lie directly on the pre-eruption surface below fall deposits of ash and fine lapilli. But elsewhere, a scattering (section C) to thin layer (sections D and M) of pumice lies above a basal gray ash and is overlain directly by the

scoria-fall deposit. We don't know if this complexity originates from eruption of pumice both before and after eruptions that deposited the ash and fine lapilli unit or if it is a result of restricted deposition and (or) differential erosion of the thin units emplaced during the early stages of the eruption. We suspect the latter, because nowhere do we see a sequence of two pumice beds separated by a gray, ash-and-fine lapilli, fall deposit.

[Figure 4 near here]

Scoria-fall deposit

The andesitic scoria-fall deposit reaches a maximum observed thickness of about 1 m on the upper east flank (Set 2 of Self and others, 1989; Fig. 2, Section A). At sites 5 to 10 km from the crater rim, thickness is typically 35 to 60 cm, except on the southwest flank where only about 5 to 10 cm is present (Fig. 3C). The restricted land area in which the deposit is preserved makes construction of isopachs difficult, but the thickness data indicate dispersal chiefly to the north and east. Limited data on clast size are also consistent with such a pattern. Mean-maximum diameter of the five largest scoria clasts at sites 5 to 10 km north and east of the caldera rim are typically 10 to 20 cm, whereas they are about 5 cm at a similar distance to the south and west. Mean-maximum diameter of dense lithic clasts is about 5 to 10 cm at sites to north and east and about 2 to 5 cm to the south and west. As observed by Williams (1952), much of the scoria-fall deposit has been eroded from the upper flanks. Early observers noted that tropical rains created marked changes in just two years following the eruption (Roberts, 1924, p. 206-207).

Pyroclastic flows and surges that followed the scoria fall were probably also effective in scouring earlier fall deposits on the upper slopes.

In most localities the scoria-fall deposit is composed of a single massive bed of lapilli with a brown base and dark-gray top (Fig. 4). Clasts are dominantly angular to subangular and display a wide range in vesicularity—from frothy scoria to dense, fresh fragments with few vesicles. Variably hydrothermally altered accidental clasts locally make up several percent of the unit. Reverse grading is evident locally, with an ash-rich base and the coarsest clasts about two-thirds up from the base, but grading is quite variable overall. In some localities the scoria-fall deposit is capped by a few centimeters of gray scoriaceous ash (e.g., Fig. 2, section L; Fig. 4). If not buried by deposits of pyroclastic surges or flows, ash clouds, or lahars, the scoria-fall deposit is typically preserved below tens of centimeters of colluvium and soil derived from reworking of 1835 deposits.

Chemical analyses of five andesitic clasts from the scoria-fall deposit range over 2.4 wt.% SiO₂ (57.4 to 59.8 wt.% SiO₂; Table 1; Fig. 5), but show no systematic relationship to color, which appears to be a function of greater vesicularity in the brown clasts. **CAG-**
-More about chemistry, density, vesicularity, color, etc.? A compositional gap of about 3 wt.% SiO₂ separates the andesitic scoria from the earlier dacitic pumice.

Self and others (1989) describe flows of andesitic agglutinate that cover portions of the caldera rim and upper flanks. Samples from near the rim have compositions (58 wt.%

SiO₂) in the mid-range of analyses of 1835 andesitic scoria (Table 1, samples 9 and COS3; agglutinate samples are plotted as fall deposits in Fig. 5). The agglutinate is exposed mostly at the surface on steep eroding slopes and is locally overlain by thin coarse-grained deposits that could be colluvium or a lag from pyroclastic flows. Nowhere have we seen below the agglutinate to judge its stratigraphic position with respect to the scoria fall or other deposits of 1835.

[Figure 5 near here]

Deposits above scoria-fall deposit

Over much of Cosigüina's lower flanks, the scoria-fall deposit lies below a mantle of sediments related to pyroclastic flows or to rapid erosion of eruptive deposits during subsequent rainy seasons and their redeposition as lahar and alluvial sediments.

Deposits of pyroclastic flows and surges composed of scoria, dense juvenile and accidental clasts, and ash overlie the scoria-fall deposit at numerous sites on the southeast, east, north, and northwest flanks (Fig. 2, sections J-M; Williams, 1952; Self and others, 1989). They form several broad fans and narrower valley fills on the lower flanks (Fig. 6). The pronounced arcuate ridge west of the crater evidently diverted most of the flows in the western sector northwestward and perhaps southward. The largest fan forms the broad, gently sloping surface west of the village of Cosigüina. Nearby Hacienda Cosigüina was reportedly buried by 6 to 7 m of material in 1835 (Roberts, 1924). Outcrops within a few kilometers upslope of the hacienda site expose as much as

4 m of dark-gray to pinkish- and brownish-gray pyroclastic-flow deposits with no base visible. Lesser thicknesses are exposed above the scoria-fall deposit (Fig. 2, section E), and some low broad ridges that rise a meter or two above the general level of the fan surface have only a thin (tens of centimeters) veneer of ash-cloud-surge deposits above the fall deposit. Such a distribution suggests that the flows in these reaches were relatively sluggish.

Distal surfaces of the fan north and south of the village of Cosigüina are composed of alluvial sand and gravel at least several meters thick derived from erosion of the pyroclastic-flow deposits. How far the pyroclastic flows extended originally in these distal areas is not known. But the low-relief area of swamps, salt marshes, and mangroves farther east is within a few meters of sea level and was likely at or below sea level prior to the eruption and subsequent alluviation. Caldeleugh's (1836) description of the eruption drawn from eyewitness accounts mentions that the shore was extended by about 250 m, but the timing of such observation is uncertain and may have followed some reworking of the deposits seaward. Therefore, the pyroclastic flows may not have traveled very far east of the village of Cosigüina, a total distance of about 10 km from the 800-m-high caldera rim. Pyroclastic-flow deposits that form the small fans and valley fills south and northwest of Potosí are poorly exposed, but thin pyroclastic-flow and ash-cloud-surge deposits overlying the scoria-fall deposit mantle intervening broad ridges.

[Figure 6 near here]

Gray to black prismatically jointed and bread-crusteds bombs (Table 1, sample 8) up to 1 m in diameter are scattered throughout the pyroclastic-flow deposits west of the village of Cosigüina and can be traced locally as high as 550 m on the upper south flank. Two small cinder cones, Cerros Chachos, whose bases lie at about 250 m, were scoured by the flows into slightly streamlined forms. Locally the deposits contain abundant charcoal, ranging from small fragments to entire logs. A small, charcoalized twig in basal pyroclastic-surge deposits between the scoria-fall and pyroclastic-flow deposits in section E yielded a radiocarbon age indistinguishable from a modern age, as would be expected for a deposit dating from 1835 (Table 2).

Sea cliffs along the Gulf of Fonseca provide excellent exposures through the pyroclastic-flow fan on the northwest flank (Fig. 2, sections I-L; Fig. 7). Maximum exposed thickness of 1835 pyroclastic-flow deposits is about 12 m with no base visible within 1 m of sea level. Two massive units can be differentiated on the basis of color and texture (Fig. 8). Their contact is planar and marked locally by thin, ash-rich, surge and fall deposits. The lower directly overlies the scoria-fall deposit or up to 1 m of intervening scoria-rich pyroclastic-surge deposits and is dark gray to black. The upper unit, which has a distinctly browner matrix owing to a greater content of fine-grained matrix, also contains black scoriaceous clasts similar to those in the lower unit. It almost everywhere lies above the dark-gray unit except on the higher portions of the pre-1835 surface that stood above the reach of the dark-gray flows (Fig. 7). There it overlies 1835 scoria-fall deposits mantling the older surface. At both ends of the coastal exposures shown in

Figure 7, the base of the pyroclastic-flow deposits descends to some unknown depth below present sea level.

[Figure 7 near here]

[Figure 8 near here]

Both the dark-gray and brown pyroclastic-flow deposits exposed along the cliffs must have originally extended some distance beyond the present shore. Extrapolation of the fan slope beyond the cliff suggests that the pyroclastic-flow deposits may have extended at least several hundred meters farther out into the Gulf of Fonseca, which in this region has a gently sloping bottom. Present depths 2 km offshore range from 6 to 10 m.

Reports of eyewitnesses who visited the northwest coast by boat on February 9, two weeks after the eruption, describe the destruction of the old-growth forest that mantled the volcano's slopes and the appearance of shoals and two low islands composed of pumice (Galindo, 1835b). A broad wedge of sediment topped by the spit of Punta San José, which is composed of sand eroded from the pyroclastic-flow and younger deposits, was formed as the sea cliff retreated.

Elsewhere, especially on the southwest flank (Fig. 2, sections F-H), which was protected from long-traveled pyroclastic flows by the prominent arcuate ridge west of the caldera, the scoria-fall deposit is overlain by light-gray to light-grayish-brown, laminated to thinly bedded ash-fall deposits locally more than 1 m thick (Fig. 3D). Accretionary lapilli up to 1 cm in diameter are common throughout the ash deposit, in places as beds with little

matrix (Fig. 9). The lapilli typically have cores of coarse dark-gray scoriaceous ash and rims of light-colored very-fine-sand- and silt-sized ash. Similar deposits, typically a few tens of centimeters to almost one meter thick, overlie pyroclastic-flow deposits along the northwest coast and northern flank. We interpret the ash as having originated in at least three ways. Owing to its close stratigraphic relation with pyroclastic-flow deposits and the similar appearance of the ash cores and silty rims to components of those deposits, we think that most originated from ash clouds elutriated from moving pyroclastic flows. The ash was dispersed by prevailing tropospheric winds primarily southwestward.

Pyroclastic flows entered the sea broadly along the northwest coast and perhaps in places along the north, northeast, and southeast coasts. Explosions driven by interaction of the hot deposits and seawater may also have produced copious ash clouds (e.g., Walker, 1979). In addition, historical accounts of several days of waning ashfall after the eruption climaxed may have contributed low-altitude ash plumes that were dispersed mainly southwestward.

[Figure 9 near here]

Hradecky and others (2001) map deposits of pyroclastic flows and surges of 1835 along the entire Pacific coast on the southwest flank of the volcano. Our work shows that from section F to G (Figs. 1, 2), between Apascali and Punta Ñata, deposits of 1835 are limited to basal-ash and fine-lapilli fall deposits, thin scoria-fall deposits, and a meter-thick overlying sequence of fine-grained fall deposits. We find that the broad coalescing fans ending in high cliffs above the Pacific Ocean are composed of volcaniclastic sediments of

varied ages and origins—chiefly lahar and alluvial. The arcuate ridge west of the caldera and the low range of hills, including Loma El Ojochito, to the south were able to deflect 1835 pyroclastic flows away from the southwest flank.

The chemical compositions of gray scoriaceous bombs from pyroclastic-flow deposits are similar to those of lapilli in the scoria-fall deposit (Table 1; Fig. 5). Samples came from both the dark-gray and brown deposits and from the major fans in the northwest and southeast sectors. We found none of the dacitic white to light-gray pumice, common in the basal part of the 1835 eruption sequence, in the pyroclastic-flow deposits.

A mantle of diamicts and alluvial deposits locally more than 5 m thick overlies the pyroclastic-flow deposits along most of the northwest coast (Figs. 2, 7, 8B, and 10). We infer that they are related to erosion of the pyroclastic-flow deposits and steep upper flanks of the volcano in the years immediately following the eruption. Roberts (1924), who visited the area in the early 20th century, reports that the descendants of the man who ran Hacienda Cosigüina in 1835 said that after two rainy seasons the land was again well vegetated and agriculturally productive and the people who fled returned. As witnessed at Mount Pinatubo after the 1991 eruption, the erosion of pyroclastic-flow deposits and deposition of lahar and alluvial fans was most rapid during the first few years and declined substantially thereafter (Janda and others, 1996).

[Figure 10 near here]

Pumice rafts?

Contemporary accounts of pumice rafts from Cosigüina encountered by ships at sea are perplexing. The two reports most often cited are secondhand. Caldcleugh (1836) relates the observations of a British captain who sailed for 65 km through floating pumice, some of which was of “considerable size”, 1800 km southwest of Cosigüina. Unfortunately, the date of the encounter is not given (Caldcleugh’s report was written about 7 months after the eruption). Squires (1851) was informed by a ship’s captain who sailed by the volcano a few days after the eruption that the sea for about 50 leagues (250 km) was covered with a near-continuous mass of pumice. It is unclear whether this was the Pacific Ocean, the Gulf of Fonseca, or both. We find little floatable pumice in the 1835 sequence on land, other than a portion of the dacitic pumice bed in basal deposits seen chiefly along the northwest coast, and wonder if these reports are accurate and even if the distal raft originated from Cosigüina.

Other reports from ships passing the Pacific coast (e.g., Galindo, 1835b) describe darkness and fall of fine-grained ash (“copious showers of dust”), not the pumice lapilli or bombs needed to form a pumice raft. Such reports are consistent with the types of deposits we find along the Pacific coast, namely fine-grained basal ash and fine lapilli and the thicker upper unit of ash deposits related largely to pyroclastic flows.

Galindo (1835b) translated a report written by the commandant of the port of La Unión, El Salvador, which lies across the Gulf of Fonseca from the volcano, about the findings of a group who visited the shore northwest of Cosigüina just two weeks after the

eruption. They describe shoals and small islands of pumice beyond the former shore, but make no mention of floating pumice rafts. If there were conspicuous pumice rafts present in the Gulf of Fonseca, which was the focus of both pumice and scoria falls and pyroclastic flows, it is remarkable that no mention is made of them, especially considering that the gulf was an important means of travel among El Salvador, Honduras, and Nicaragua.

If the eruption produced large pumice rafts, there are only limited deposits on land that could represent potential sources. The scoria clasts in the fall and pyroclastic-flow deposits are almost all denser than water. The dacitic pumice-fall deposit contains a floatable fraction, but the entire bed is typically only a few centimeters thick except in a narrow segment along the coast northwest of the volcano. If the dacitic bed is the source, the raft must have originated in the Gulf of Fonseca north of the volcano and then drifted into the Pacific. The Gulf is about 35 to 50 km wide, but the only reports of pumice fall were from Isla El Tigre, about 20 km away, where pea- to hen's-egg-sized clasts were noted on 21 January (Galindo, 1835a). Could such a raft be 250 km wide off the Pacific coast or 65 km wide 1800 km away? Did the eyewitness reports exaggerate the size of the rafts? Certainly many other reports related to the eruptions were exaggerated (e.g., Self and others, 1989). Was the 1800-km-distant raft even related to the Cosigüina eruption? At present these issues cannot be resolved.

Volume of 1835 eruptive products

Estimates of the volume of tephra-fall and pyroclastic-flow deposits emplaced by the 1835 eruption have varied over several orders of magnitude. Self and others (1989) describe how volume estimates of $\geq 50 \text{ km}^3$ in the decades following the eruption must represent erroneous reporting. Almost none of the 19th century reports, except for a few of ashfall from distal sites, are firsthand accounts. Widely repeated reports of 5 m of dust accumulating for more than 40 km from the volcano are clearly absurd. At such a distance several reliable descriptions note uncompacted tephra fallout of, at most, 10 to 20 cm.

We searched for Cosigüina tephra in eastern El Salvador, but we turned up no sites with recognizable deposits. We concentrated in areas near San Miguel and La Union, which, according to eyewitness reports, received 10 cm or more of uncompacted ash (Galindo, 1835a, b). We found several basin and floodplain localities with well-preserved fine-grained white ashfall deposits up to 25 cm thick that are distal fallout of the A.D. 430 eruption of Ilopango caldera, near San Salvador, on the basis of radiocarbon age and bulk chemistry (Escobar, 2003; Dull, 2004). In many of these sites, the original fall deposit was immediately buried in alluvium or colluvium of reworked ash, thereby ensuring its preservation. None of the areas we checked that provided good traps for the Ilopango ash had any sign of a younger deposit that could be distal tephra of the 1835 Cosigüina eruption or its reworked equivalent. A key question to us is how accurate are the tephra thicknesses reported by 1835 eyewitnesses. Perhaps exaggerated reports by terrified residents and the low bulk density of newly fallen tephra contributed to overly large

estimates of the amount that fell. Coring in lakes, the Gulf of Fonseca, or coastal wetlands is probably the only way to ultimately gain confidence in accurate distal thickness estimates.

Our proximal data on thickness of the scoria-fall deposit (Fig. 3C) suggest that the circular isopachs constructed by Self and others (1989, Fig. 1) are too generous and that deposition from the climactic scoria-fall was dominantly toward the northwest to northeast. For example, 10-cm thicknesses of climactic fine scoria and ash along the southern flank of the volcano (e.g., Fig. 2, Sections F and G) lie about 30 km inward of their 10-cm isopach. Thicker fine-grained fall deposits that lie below and above the climactic fall in this area originated from low-altitude eruption plumes and from ash clouds of pyroclastic flows and therefore cannot be combined with the climactic fall for purposes of extrapolating distal thickness. In addition, the data in Figure 3C allow estimation of a 50-cm isopach for the scoria-fall deposit that encompasses about 180 km², which is roughly 10% of the area estimated from Self and others (1989; Fig. 4). If the area of Self and others' (1989) circular 10- and 5-cm isopachs are reduced by about one-half, the bulk volume could be roughly one-half of their 4.1 km³ estimate.

Great uncertainties about amounts of distal tephra confound attempts to further refine estimates of the total bulk volume of tephra from the climactic scoria fall, but our reconnaissance mapping provides broad limits on the volume of pyroclastic-flow deposits. Lack of exposures make thickness estimates difficult, but a rough bulk-volume estimate is 0.5 to 1 km³ (110 km² covered with a mean thickness of 5 to 10 m). Fine-

grained ash-fall deposits associated with pyroclastic flows and waning stages of the eruption (Fig. 3D), whose distal extent in the Pacific Ocean is unknown, could add a few additional tenths of a cubic kilometer.

Our minimum estimate of the total bulk volume of eruptive products emplaced in 1835 is pyroclastic-flow deposits, 0.5 km^3 , fine-grained proximal ash-fall deposits, 0.2 km^3 , scoria-fall deposit 2 km^3 (excluding Self and others (1989) estimate of 1.5 km^3 of distal ash-fall deposit), for a total of roughly 3 km^3 . Distal ash could add one or more cubic kilometers, but, as mentioned above, the uncertainties are too great to warrant further refinement. The 1902 eruption of Santa María in Guatemala was probably the only eruption in Central America during the past few centuries that produced a greater volume of ejecta—about 7.8 km^3 (Fierstein and Nathenson, 1992).

PRE-1835 DEPOSITS

In addition to the widely reported eruption of Cosigüina in 1835, Simkin and Siebert (1994) list eruptions of uncertain magnitude and date in A.D. 1500 and 1709, an uncertain eruption in 1609, and eruptions, probably small, in 1809, 1852, and 1859. Feldman (1993, p. 235) notes that little mention is made about Cosigüina prior to 1835 in the colonial archives of the former port, naval base, and provincial capital of Realjo (founded in 1633 near present-day Corinto), which was located about 65 km from the volcano. If the volcano did erupt in the two centuries before 1835, the eruptions must

have been nothing near the scale of the 1835 event, which was chronicled at length owing to local tephra fall, darkness, striking views of the eruption column, and loud eruption sounds. The records of other nearby cities such as El Viejo and Leon in Nicaragua and San Miguel in El Salvador, which were settled even earlier than Realjo and clearly were affected by the 1835 eruption, likewise have no mention of earlier eruptions of Cosigüina. In this section we describe briefly the tephra and flowage deposits of older eruptions of Cosigüina that we see locally exposed below the deposits of 1835.

A recent geologic map by Hradecky and others (2001) delineates products of Cosigüina and older rocks. The upper part of the cone includes a pronounced arcuate rim to the west of older lavas. To the east, Loma San Juan is a strongly weathered remnant of an older andesitic volcano; to the south is low terrain underlain by volcanic rocks and sediments of the Tertiary Coyoil Formation. They map several units of recent pyroclastic deposits as extensive as, or more so, than those of 1835 that they assign to eruptions around A.D. 1500 and 1700. Two other eruptive sequences are noted between these. As discussed below, we interpret the record differently.

In sea-cliff exposures along the northwest coast (Figs. 2, 7, 10), pyroclastic-fall and -flow deposits of 1835 bury older diamicts and alluvium that resemble the lahar and alluvial deposits emplaced following the 1835 eruption. The clasts in the pre-1835 diamicts are subangular to round and composed of varied lava types. The diamicts range from matrix to clast supported and contain charred and uncharred wood fragments. One charred fragment yielded a 2-sigma, calibrated radiocarbon age range of A.D. 1400 to 1470 (Fig.

2, section K; Table 2). A rock type that appeared fresh and incipiently prismatically jointed is a basaltic andesite (Table 1, sample 2; 55 wt. % SiO_2), more mafic than products of 1835. Few of the diamicts look like primary pyroclastic-flow deposits and likely are chiefly deposits of lahars produced by erosion immediately following an older eruptive period. In the area between sections I and J, the diamicts terminate in an exhumed ancient sea cliff that was buried by 1835 deposits.

At several sections, scoria-fall and pyroclastic-flow deposits underlie deposits of 1835, separated by a weak buried soil several tens of centimeters thick (Fig. 2; sections A-D, G, H, and M). The buried soil probably represents no more than a few centuries of surface exposure. Except at section M, the pre-1835 deposit is solely a uniform to slightly graded fine-lapilli scoria-fall deposit. Nothing like the 1835 fine-grained basal tephra or accretionary-lapilli-rich deposits are present. Nowhere is the older scoria-fall deposit coarser-grained than the overlying 1835 scoria-fall deposit. These scattered observations imply that the pre-1835 eruption was of lesser magnitude than that of 1835. Broadly contemporaneous pyroclastic-surge and -flow deposits overlie the pre-1835 scoria-fall deposit in section M, but nowhere have thick pyroclastic-flow deposits on the order of several hundred years old and comparable in character to those of 1835 been found. They could be buried under flowage deposits of 1835 whose base is not exposed, but the lack of accretionary-lapilli-rich ash-cloud deposits suggests that there were not significant pyroclastic flows produced during this penultimate eruption. Clasts from the pre-1835 scoria-fall deposit contain about 57 wt % SiO_2 ; slightly more mafic than the most mafic clasts from 1835 deposits (Table 1, samples 3 and 4; Fig. 5). We have no direct

stratigraphic evidence to link these scoriaceous deposits with the 15th (?) Century diamicts exposed in section K, but the degree of soil development between 1835 and pre-1835 scoria-fall deposits suggests the latter could be broadly time correlative with the diamicts.

Tens of pyroclastic-fall and pyroclastic-flow deposits are exposed along the trail that descends steeply from section H to the coast in an area called Tigüilotada (Figs. 1, 2). The pre-1835 scoria-fall deposit in section H is underlain by about 4 to 5 m of fine-grained colluvium that contains numerous buried soils, some of which have argillic B horizons. This sequence of sediments and soils must represent at least several thousand years. Such an interpretation is markedly different from that of Hradecky and others (2001), who map the deposits in this area as all younger than A.D. 1500 (their Sequencias II to V). But such an interpretation is difficult to justify in light of the soil evidence. A scoria-fall deposit within the sequence of colluvium and soils is barely andesitic (53.2 wt % SiO₂; Table 1, sample 1). Below, the section is dominated by pumice-fall deposits, diamicts, and alluvial deposits. A conspicuous, compositionally graded, 1.6-m-thick pumice-fall deposit (probably pumice unit EP of Hradecky and others, 2001) about one-third of the way to the beach (UTM 0427346E/1433493N) has a light-gray dacitic (64.8 wt % SiO₂) base and dark-gray andesitic (57.5 wt % SiO₂) top, which closely mimics the range of compositions seen in the 1835 eruptive sequence (Table 1; Figs. 5, 11). In total the section records more than 10 sizable tephra-fall eruptions, the deposits of which are all thicker and coarser than those of 1835 in section H. Unfortunately there is no numerical age control in the section, but the lack of prominent weathering horizons and

marked disconformities in the lower part suggests that it was deposited fairly continuously prior to a hiatus of at least several thousand years as indicated by the colluvial unit with buried soils.

[Figure 11 near here]

We have additional differences with the map by Hradecky and others (2001), chiefly related to their interpretation of stratigraphic relations in sea cliffs along the northwest coast and to the age and extent of pyroclastic-flow deposits in fans on the lower southeast flank of Cosigüina.

[Table 2 near here]

Our interpretation of the northwest coastal exposures is guided by tracing the scoria-fall deposit of 1835 around the volcano and by radiocarbon ages of charcoal within the overlying pyroclastic-flow and surge deposits (Figs. 2, 7; Table 2). Our two radiocarbon samples that have ages indistinguishable from modern are small charcoaled twigs from surge deposits. The scoria-fall deposit mantles a dissected landscape formed chiefly in lahar and alluvial deposits. The overlying 1835 pyroclastic-flow deposits are thick in former valley bottoms and are thin or absent on former ridge tops, extend to the face of the sea cliff, and no doubt reached at least several hundred meters more seaward before being eroded back. In contrast, Hradecky and others (2001) map several units in this same area—pyroclastic-flow and surge deposits of A.D. 1500 (UH1), 1700 (UH2), and

an intervening episode—depicted as roughly beach-parallel polygons. We don't see the stratigraphic evidence to support this interpretation. In addition, we don't know the localities from which their ages came, but the great uncertainties during the past 500 ^{14}C yr imparted by variations in the calibration curve create poor age resolution. At 95%-confidence level (and even at 1- σ level), the ages for units UH1 and UH2 of Hradecky and others (2001) overlap and provide only broad age constraints of several centuries. It is impossible to assign UH1 to 1500 and UH2 to 1700 on the basis of these ages. Some of the spread in ages may be due to sample selection. There are numerous large, probably long-lived, charred trees in the pyroclastic-flow deposits that could provide material that ranges in age over several centuries.

Table 2. Radiocarbon ages from deposits of Cosigüina. Calibration by methods described in Stuiver and Rymer (1993). Hradecky and others (2001) did not publish the laboratory numbers of their samples, which here are labeled CU-unk.

Laboratory number	Age BP, in ^{14}C yr $\pm 1\sigma$	Calibrated age, A.D. 1- σ range	Calibrated age, A.D. 2- σ range	Stratigraphic position assigned in reference	Reference
Beta-177981	modern	NA	NA	1835 surge deposits, sec L	This report
Beta-177982	30 ± 50	NA	NA	1835 surge deposits, sec E	“
Beta-177983	490 ± 50	1410-1440	1400-1470	Pre-1835 diamicts, sec K	“
CU-unk (Prague)	295 ± 121	1448-1676, 1775-1802*	1428-1887*	Deposits of 1700 or 1709 eruption, UH2	Hradecky and others (2001)
CU-unk (Prague)	310 ± 127	1441-1675, 1776-1801*	1414-1887*	“	“
CU-unk (Prague)	330 ± 128	1438-1669*	1402-1887*	“	“
CU-unk (Prague)	374 ± 128	1428-1651	1384-1813*	“	“
CU-unk (Prague)	430 ± 128	1405-1636	1289-1679*	“	“
CU-unk (Prague)	505 ± 127	1300-1494*	1262-1659	Deposits of 1500 eruption, UH1	“
CU-unk (Prague)	506 ± 127	1299-1494*	1262-1659	“	“
CU-unk (Prague)	498 ± 128	1302-1515*	1262-1664*	“	“

* Excludes extreme values that have <5% probabilities in calibration results

Hradecky and others (2001) show pyroclastic-flow deposits of 1835 extending only about 6 km southeastward from the caldera rim; more distal deposits are assigned to eruptions in about A.D. 1700. Section E (Fig. 2), which is located in the latter area, exposes the typical 1835 sequence of scoria-fall deposit overlain by pyroclastic-flow and surge deposits from which we have a modern radiocarbon age. This sequence is traceable over a broad area of the southeast fan in both areas mapped as deposits of 1700 and 1835 by Hradecky and others (2001). In addition, Hacienda Cosigüina, which is located within the pyroclastic-flow deposits ascribed to 1700, “was buried under 21 feet of drift” during the eruption (Roberts, 1924, p. 206-207). Clearly, the pyroclastic-flow deposits exposed in the southeast sector date from 1835.

DISCUSSION

As outlined above, the great Cosigüina eruption of 1835 followed a century or more of relative quiescence; probably at least several millennia had elapsed since a period of frequent eruptions of similar or greater magnitude than that of 1835. The form of the volcano and its caldera at the start of the 1835 eruption is not well constrained by observations, so we don't know what conditions were like and whether or not a lake occupied the vent. Contemporary reports following the eruption make no mention of radical changes in the profile of the cone, three sides of which were clearly visible to mariners, so perhaps the shape of the outer cone was little changed.

Self and others (1989) suggested correlations between their three-fold sequence of deposits on the upper east flank of the volcano and reports of eyewitnesses. We mostly agree with their interpretations, but add a few points below.

Phase 1 (following the nomenclature of Self and others, 1989)

The growth of an eruption column between 06:30 and 08:00 (all local time) on 20 January was followed a few hours later by ash fall at La Union, El Salvador, about 50 km north-northwest of Cosigüina, and at Nacaome, Honduras, about 60 km north. Basal ash and dacitic pumice-fall deposits in sections K, L, and M (Fig. 2) on the northwest to north flanks of the volcano lie directly on soil and older deposits and must be related to this

initial explosive eruption that lasted throughout the day. The “phosphoric sand” that fell in La Union from 16:00 to 20:00 (Galindo, 1835b) may be the distal equivalent of the dacitic pumice fall, which is the coarsest-grained of the basal deposits. The transport of tephra northward is consistent with high-altitude (>6 km) winds during January. Thin fine-grained basal ash present in south, southeast, and east sectors (sections B to F, Fig. 2) and thicker and coarser basal ash and fine lapilli in the southwest and west (sections G and H) are consistent with southwestward transport by low-altitude, tropospheric winds.

Phase 2

A brief lull during the night of 20-21 January was followed by vigorous eruptive activity beginning on the morning of 21 January. Lapilli the size of peas to hen’s eggs fell on Isla El Tigre, 35 km north-northwest of Cosigüina (Galindo, 1835b). This represents the coarsest distal fall material reported during the eruption and most reasonably correlates with the main scoria fall that is prominent on all flanks of the volcano. During both phases 1 and 2, reports from the southeast, including Realjo and nearby San Antonio (both near present-day Corinto), describe dramatic views of the eruption cloud, but no local ash fall. High-altitude winds continued their dominant northward and northeastward transport of tephra.

Phase 3

From 22 to 24 January, and perhaps through the end of the month, ash fall spread southeastward to cover most of western Nicaragua. Intermittent ash fall was also reported in La Union and other parts of eastern El Salvador. Self and others (1989)

postulated a shift in high-altitude winds in at least some altitude bands during this time period to promote the southeasterly dispersal of ash. Concurrently ships off the Pacific coast were also enveloped in ash fall. The most reasonable explanation to us is that explosions spawning pyroclastic flows and lower-altitude eruption columns characterized at least part of this time period. Thick, accretionary-lapilli-rich ash-fall deposits on the southwest flank (Fig. 9) in part represent ash clouds of pyroclastic flows that were transported by the prevailing tropospheric winds to the southwest.

Deposits of the 1835 eruption record a variety of volcanic processes. Initial events that were accompanied by loud explosions produced chiefly tephra-fall deposits. These included ash and fine-lapilli falls that may have been accompanied by areally restricted surges described by Self and others (1989) on the upper east flank. Such falls probably were related to relatively low (<6 km) eruption columns. The modest dacitic pumice fall of probable subplinian character and the subsequent extensive andesitic scoria falls were produced by higher (>6 km) eruption columns. The dacitic pumice, which is distinctly more silicic (by 3 to 6 wt%; Table 1, Fig. 5) than the andesite probably represents a small volume of more differentiated magma that was residing at a shallower level and erupted early. The andesite is the most voluminous component and on the basis of the relatively simple character of the scoria-fall deposit was evidently emplaced at a fairly constant rate. Early, more inflated brown scoria was rather abruptly replaced by a dark-gray scoria that was denser and included some nearly vesicle-free juvenile material. The lack of interbedding of scoria-fall and -flow deposits suggests another abrupt transition, this time to low collapsing columns or fountains of scoria that fed pyroclastic flows down all

flanks of the volcano. Elutriation of ash from the flows produced thick deposits of accretionary-lapilli-rich ash, especially to the southwest where low-altitude winds would concentrate such deposits. The possible presence during all or part of the eruption of a caldera lake, similar to present-day conditions, suggests that surface or shallow ground water may have played a role in quenching some of the magma to produce higher densities and some of the profound explosions that were heard at great distances.

PRELIMINARY HAZARDS ASSESSMENT

During historical time (past ~500 yr), Volcán Cosigüina has erupted much less frequently than many of the other volcanic centers in northwestern Nicaragua, such as Momotombo, Telica, or San Cristobal (Fig. 1). But the 1835 eruption of Cosigüina was by far the most significant in terms of explosivity, extent of pyroclastic flows, and volume of tephra fall. As described above, the penultimate eruption of consequence may date from the 15th Century, prior to European settlement. The poorly dated prehistorical record of the volcano, as viewed in the Tigüilotada section, suggests that up to tens of large, explosive eruptions of andesitic to dacitic magma occurred during the recent geologic past, but prior to several thousand years ago. This record of infrequent, but sizable eruptions indicates that, if Cosigüina becomes restless, it should be regarded as capable of producing an eruption on the order of that of 1835, or even somewhat larger.

We use the mapped extent of pyroclastic-flow and -surge deposits of 1835 (Fig. 6) as a guide for establishing a proximal hazard zone for future such events (Fig. 12). In future eruptions the arcuate ridge on the upper west flank of the volcano will probably divert pyroclastic flows as it did in 1835. Its relatively modest height (≤ 200 m) suggests that energetic flows and surges could surmount the ridge and concentrate in the small valleys that trend west and northwest from the ridge. The major fans and valley fills of 1835 pyroclastic-flow deposits are the most likely paths for future flows. The east end of Loma San Juan was not subjected to pyroclastic flows in 1835, but it was possibly swept by ash-cloud surges and is close enough to the vent (8 to 9 km) as to not offer much refuge. Pyroclastic flows did not reach the southwestern coast in 1835, nevertheless the region from Apascali to Punta Ñata received thick falls (>1 m thick prior to settling and compaction) from ash clouds of pyroclastic flows and vent explosions. Movement of vehicles would probably be impossible under such conditions. It was probably a very unpleasant environment during and after the eruption as winds resuspended the fine ash during dry periods or as rain saturated the fine ash to form deep mud. Roofs of buildings over most of the peninsula surrounding Cosigüina would be vulnerable to collapse from tephra loads of the thicknesses that accumulated in 1835, especially if the eruption were accompanied by heavy rain.

[Figure 12 near here]

Cosigüina's location on a peninsula, with only one major road allowing rapid evacuation to a distance greater than 15 km from the vent, reduces the options for risk mitigation for

the ~5000 residents of the peninsula and their herds of livestock. Peninsula Venecia and small roads that head east along the mangroves on the south shore of the Gulf of Fonseca provide other limited routes, but the potentially severe impacts of a repeat of an 1835-scale eruption probably make evacuation of the peninsula prior to onset of an eruption the best measure to protect humans and livestock. Relatively densely populated areas near the villages of Cosigüina, Potosi, and along the road from Potosi to El Rosario are all at risk from pyroclastic flows and surges. The areas at least risk from pyroclastic flows are likely to be along the Pacific coast southeast of Apascali.

From observations of witnesses in the aftermath of 1835 and experience at other eruptions, a period of rapid sediment production and unstable channels as drainage networks reestablish on the new landscape would follow a significant eruption. Low areas downstream from pyroclastic-flow deposits would be most affected, but widespread tephra fall could also trigger high sediment loads in watersheds unaffected by pyroclastic flows. The broad fans on the southeast and north would likely grow and extend farther into the sea or fringing mangroves.

The distribution of tephra fall during future eruptions will be controlled by characteristics of the eruption (volume, column height, etc.) and wind direction and strength (Fig. 13).

The eruption of January 1835 illustrates tephra fallout under typical dry-season (December through April) wind conditions. Low-altitude (<6 km) winds are chiefly from the east to northeast and would carry the ash clouds of pyroclastic flows and small explosions toward Apascali, Punta Ñata, and the Pacific coast. In contrast high-altitude

(>6 km) winds blow chiefly from the west to southwest, but during the 1835 eruption must have been more southerly and carried most of the tephra to the northern sector of the volcano and to eastern El Salvador and Honduras. A shift in wind direction at higher altitudes occurred later in the eruption to account for tephra fall hundreds of kilometers to the southeast. Future dry-season eruptions that send eruption clouds above 6 km could cause similar widespread tephra fall depending on upper-level-wind patterns. During the wet season (June through October), winds below 25 km are chiefly from the east to northeast and most tephra would fall on the west to southwest flank and the Pacific Ocean. May and November are transitional months during which either wind pattern is possible.

[Figure 13 near here]

Several additional studies could help greatly in better assessing the potential hazards from future eruptions of Cosigüina.

1. Studies of cores from lakes and wetlands in Nicaragua, Honduras, and El Salvador are needed to obtain better measurements of thickness of distal tephra-fall deposits and thereby a better-controlled volume estimate for the 1835 eruption.
2. The sequence of older tephra exposed on the west flank of the volcano near Tigüilotada deserves further attention—particularly of the age and frequency of these eruptions that likely exceeded the magnitude of the 1835 event.
3. Textural and petrologic studies of 1835 and older products would improve our understanding of eruptive processes and the magmatic system.

4. Improvements in the monitoring system around Cosigüina.

Acknowledgements

Field work for this study was funded by the Volcano Disaster Assistance Program, a joint effort of the Office of Foreign Disaster Assistance of the U.S. Agency for International Development and the U.S. Geological Survey. We thank Wilfried Strauch, Dirección General de Geofísica of the Instituto Nicaragüense de Estudios Territoriales (INETER), for support and encouragement. Carlos Pullinger from the Servicio Nacional de Estudios Territoriales (SNET) of El Salvador worked with us in our futile search for Cosigüina tephra in eastern El Salvador and offered numerous insights regarding Central American volcanism. The manuscript benefited greatly from constructive reviews by Julie Donnelly-Nolan and James Vallance. His comments impacted us especially well.

References

- Caldcleugh, Alexander, 1836, Some account of the volcanic eruption of Cosigüina in the Bay of Fonseca, commonly called the Bay of Conchagua, on the western coast of Central America: *Philosophical Transactions of the Royal Society of London*, v. 126, p. 27-30.
- Dull, R.A., 2004, Lessons from the mud, lessons from the Maya; paleoecological records of the Tierra Blanca Joven eruption, *in* Rose, W.I., Bommer, J.J., Lopez, D.L., Carr, M.J., and Major, J.J., eds., *Natural Hazards in El Salvador: Geological Society of America Special Paper 375*, p. 237-244.
- Escobar, C.D., 2003, San Miguel and its volcanic hazards, El Salvador: unpublished report, Department of Geological Engineering and Sciences, Michigan Technological University, 181 p.
- Feldman, L.H., 1993, Mountains of fire, lands that shake—earthquakes and volcanic eruptions in the historic past of Central America (1505-1899): Culver City, California, Labyrinthos, 295 p.
- Fierstein, Judy, and Nathenson, Manuel, 1992, Another look at the calculation of fallout tephra volumes: *Bulletin of Volcanology*, v., 54, p. 156-167.
- Galindo, Juan, 1835a, Eruption of the volcano Cosiguina: *American Journal of Science*, v. 28, p. 332-336.
- Galindo, Juan, 1835b, On the eruption of the volcano Cosigüina, in Nicaragua: *Journal of the Royal Geographical Society of London*, v. 5, p. 387-392.
- Gardner, C.A., Scott, W.E., Ewert, J.W., Griswold, J.P., Cunico, M.L., and Devoli, G., 2004, Hazard assessment for Volcán Telica, Nicaragua: U.S. Geological Survey Open-File Report 2004-1046, 24 p.
- Hradecký, P., Havlicek, P., Opletal, M., Rapprich, V., Sebesta, J., Sevcik, and Mayorga, E., 2001, Estudio geológico y reconocimiento de amenazas geológicas en el Volcán Cosigüina, Nicaragua: Servicio geológico de la República Checa (CGU) and Instituto Nicaragüense de Estudios Territoriales (INETER), 42 p.
- Janda, R.J., Daag, A.S., Delos Reyes, P.J., Newhall, C.G., Pierson, T.C., Punongbayan, R.S., Rodolfo, K.S., Solidum, R.U., and Umbal, J.V., 1996, Assessment and response to lahar hazard around Mount Pinatubo, 1991 to 1993, *in*, Newhall, C.G., and Punongbayan, R.S., eds., *Fire and Mud: Eruptions and lahars of Mount Pinatubo*, Philippines: Quezon City, Philippine Institute of Volcanology and Seismology, and Seattle, University of Washington Press, p. 107-139.

Johnson, D. M., Hooper, P. R., and Conrey, R. M., 1999, XRF analysis of rocks and minerals for major and trace elements on a single low dilution Li-tetraborate fused bead: *Advances in X-ray Analysis*, vol. 41, p. 843-867.

Roberts, Morely, 1924, *On the earthquake line: Minor adventures in Central America*: London, Arrowsmith, 309 p.

Self, S., Rampino, M.R., and Carr, M.J., 1989, A reappraisal of the 1835 eruption of Cosigüina and its atmospheric impact: *Bulletin of Volcanology*, v. 52, p. 57-65.

Simkin, Tom, and Siebert, Lee, 1994, *Volcanoes of the World*: Tucson, Geoscience Press, 2nd edition, 349 p.

Squires, E.G., 1851, On the volcanoes of Central America, and the geographical and topographical features of Nicaragua, as connected with the proposed inter-oceanic canal: *Proceedings of the American Association for the Advancement of Science*, p. 101-122.

Stuiver, M., and Reimer, P.J., 1993, Extended ¹⁴C data base and revised CALIB 3.0 ¹⁴C age-calibration program (2002, v. CALIB 4.4): *Radiocarbon*, v. 35, p. 215-230.

Walker, G.P.L., 1979, A volcanic ash generated by explosions where ignimbrite entered the sea: *Nature*, v. 281, no. 5733, p. 642-646.

Williams, Howel, 1952, The great eruption of Coseguina, Nicaragua, in 1835: *University of California Publications in Geological Sciences*, v. 29, p. 21-46.

Figure captions

Figure 1. Shaded-relief, digital-elevation model of Volcán Cosigüina; letters show location of key stratigraphic sections (Fig. 2) and major geographic features. Summit caldera holds Laguna Volcán Cosigüina, whose surface altitude is about 160 m, more than 700 m below the highest point on the rim. The digital-elevation model was made from 1972-vintage 1:50,000-scale topographic maps (Series E751), and differs slightly from currently available maps made in the late 1980s. The roads on the DEM are especially outdated. Maps used for the DEM are Chorrera (now Peninsula Padre Ramos), Cosigüina, Estero Real, Peninsula Venecia, and Potosi. UTM grid lines are 10 km apart. Contour interval is 20 m. The dashed line marks a prominent arcuate ridge that may be an old somma rim. Much of the low-relief area around Estero Padre Ramos and east of the village of Cosigüina are low-lying mangrove swamps. Inset map shows region around Gulf of Fonseca and locations referred to in text.

Figure 2. Key stratigraphic sections (located in Figure 1) expose deposits of the 1835 eruption and earlier events. Section A and designation of Sets 1 to 3 is from Self and others (1989). Numbered boxes show stratigraphic position of chemically analyzed samples (Table 1) from sections, or from units that can be physically traced to section. X shows locations of radiocarbon-dated samples (Table 2). Sections are shown to vertical scale except where thick units are broken by jagged lines and total thicknesses are given (in meters). Pyroclastic-flow deposits of 1835 are subdivided into dark-gray (gr) and brownish-gray (br) units in those thick sequences. Alphanumeric symbols in left column of explanation refer to figures in which thicknesses of units are shown. Variation in

width of scoria-fall deposit denotes observable change in grain size; wider units are more ash rich.

Figure 3. Maps show thickness (in centimeters) of subunits of 1835 tephra-fall deposits, from bottom to top—A, lower ash to fine lapilli; B, basal to near-basal white pumice; C, main scoria fall; D, upper fine-grained, accretionary-lapilli-rich ash. Thicknesses in white circles are from lettered stratigraphic sections (Fig. 1); those in white squares are from other sites. Approximate 50-cm isopach is shown for scoria-fall deposit.

Figure 4. Basal part of 1835 deposits near section L shows white pumice-fall deposit lying directly on paleo-surface. Upper part of pumice fall is stained by iron oxides and appears dark colored. Color grading of scoria-fall deposit from brown base to dark-gray top is much more striking than appearance in this gray-tone image. Capping pyroclastic-flow deposit typically includes a stratified basal surge facies.

Figure 5. A, K_2O versus SiO_2 , and B, FeO versus SiO_2 , for deposits of 1835 eruption and older events. Analyses are listed in Table 1. 1835 fall samples include 2 samples of agglutinate lava that caps caldera rim. 1835 pyroclastic flow marked W is analysis from Williams (1952). Note the similar range in composition of 1835 deposits and those of the compositionally graded deposit (old mixed fall) exposed in the Tigüilotada area.

Figure 6. Approximate distribution of 1835 pyroclastic-flow and -surge deposits is shown by spot thickness measurements and approximate contacts that outline portions of

thick accumulations in fans (f) on the lower flanks. Pyroclastic flows entered the Gulf of Fonseca along the northwest and northeast coasts; their distal extent in the southeastern sector is poorly known owing to thick deposits of post-1835 lahar deposits and alluvium and extensive mangrove swamps. The arcuate ridge west of the summit caldera apparently diverted most flows away from west and southwest flanks, although some probably descended narrow canyons that head on the rim.

Figure 7. Generalized stratigraphic section extends along northwest coast of Cosigüina and shows how deposits of 1835 eruption buried a dissected landscape formed in older deposits. Pyroclastic-flow deposits are subdivided into lower dark-gray (gr) and upper brownish-gray (br) units. Pyroclastic-surge deposits are not differentiated from pyroclastic-flow deposits. Unit of 1835 tephra-fall deposits includes lower ash- and lapilli-fall deposits, white pumice-fall deposit, and scoria-fall deposit. Vertical lines mark sections that provide control; labeled sections are from Figure 2. Note great vertical exaggeration.

Figure 8. Photographs show typical outcrops of 1835 deposits along the northwest coast. A. The two-fold pyroclastic-flow sequence is shown overlying the pumice and scoria-fall deposits between sections K and L. Sea cliff is about 12 m high. Both pyroclastic-flow deposits (pfd) have a matrix of dark-gray scoriaceous ash, but the brownish-gray unit has a conspicuous proportion of fine-grained brownish ash that makes it browner and more cohesive. Note the fluid-escape pipes emanating from a charcoaled log. B. Dark-gray

and brownish-gray 1835 pyroclastic-flow deposits near section J are overlain by a wedge of alluvium and lahar deposits that represents a period of rapid erosion following the 1835 eruption.

Figure 9. Roadcut near Punta Ñata (section G) exposes 1835 tephra-fall deposits (photograph courtesy of Armin Freundt). The scoria-fall deposit is thinnest in this southwest sector owing to its deposition from a high eruption column and transport by southwesterly winds. The source of the upper accretionary-lapilli-rich unit is chiefly ash clouds of pyroclastic flows and is thickest in the southwest sector and close to the margin of pyroclastic-deposits in the north sector. Accretionary lapilli are up to 1 cm in diameter. The lower unit is also thickest in the southwest sector and here includes fine-lapilli throughout most of the unit above a laminated ash base.

Figure 10. Sea cliff near section K exposes a sequence of pre-1835 lahar deposits and alluvium. Cliff is about 17 m high. Charcoal from the bouldery lower pre-1835 deposit yielded a calibrated radiocarbon age of A.D. 1400-1470 at 2- σ uncertainty. The 1835 deposits include tephra-fall and pyroclastic-flow deposits and are about 3.5 m thick and are largely hidden by a bench in the upper part of the section. The 1835 deposits are less indurated than the surrounding lahar deposits and erode back to create the bench. The 3 to 4 m of slightly indurated lahar deposits and alluvium that cap the section originated by rapid erosion of deposits on the upper flanks of the volcano following the eruption.

Figure 11. Compositionally graded pumice fall deposit (white line; 1.6 m thick) exposed near Section H is much thicker and coarser grained than nearby 1835 deposits, and is one of several late Pleistocene to Holocene (?) deposits that provide evidence of eruptions of much larger magnitude in Cosigüina's past. Dashed line shows approximate location of gradational color change between white to light-gray dacitic base and gray andesitic top. Compositional range mimics that found in 1835 deposits (Table 1; Fig. 5, samples 5 and 18).

Figure 12. Preliminary hazard-assessment map for future pyroclastic flows and surges at Cosigüina based partly on mapped extent of deposits of the 1835 eruption (Fig. 6). Small arrows depict potential for small flows and surges surmounting the ridge west of the caldera (bold dashed line) and affecting terrain to the west and southwest, especially in valleys. Large arrows depict main flow paths that feed broad pyroclastic fans. Such areas are also expected to be affected by lahars and rapid alluviation following a significant eruption. Outer dashed line, which lies about 10 km from caldera rim in west and north sectors and about 15 km in south and east sectors roughly outlines area that could be affected by energetic pyroclastic surges generated by explosions and derived from pyroclastic flows. Such surges are less dense than water and could travel over the sea.

Figure 13. Wind rose diagrams for average January (dry season) and August (wet season) winds for the years 1997 to 2002 at altitudes of about 1500m and 9700 m (Gardner and others, 2004). Each diagram shows 12 segments representing a two-week

average of wind directions and speeds. Low-level wind directions (below about 6000 m) for both seasons are from the east-northeast, but high-level wind directions (above about 6000 m) differ substantially depending on season. [Will change to histograms for simplicity; no need for color.]

Table 1. Chemical analyses of products of Volcán Cosigüina. Major-element analyses are recalculated volatile-free to 100%; total Fe as FeO*. All were done by x-ray fluorescence, except for Sample W, which is from Williams (1952). Samples with COS are from Self and others (1989). Numbered samples were processed at the WSU GeoAnalytical Laboratory, Washington State University (see Johnson and others (1999) for information about technique, precision, and accuracy). Locations of sections are shown in Figure 1 and stratigraphic positions of samples from sections are shown in Figure 2.

ID#	SiO ₂	TiO ₂	Al ₂ O ₃	FeO [*]	MnO	MgO	CaO	Na ₂ O	K ₂ O	P ₂ O ₅	Ni	Cr	Sc	V	Ba	Rb	Sr	Zr	Y	Nb	Ga	Cu	Zn	Pb	La	Ce	Th	Field Sample No.	Section or Locality	UTM Coordinates 4xxxxxE/14xxxxxN	Description	
1	53.2	0.86	18.8	10.14	0.19	4.41	9.29	2.33	0.71	0.14	11	15	36	268	587	15	412	69	21	1.3	18	213	97	4	13	14	2	030211-3	150 m SSW of H	27638/33539	Old scoria fall of Tigüilotada	
2	55.3	0.75	19.1	7.97	0.18	3.06	8.47	3.88	1.05	0.20	4	2	26	198	720	19	456	92	29	1.5	19	110	87	5	12	24	2	030129-11	K	34188/39976	Clast from A.D. 1400 diamict	
3	56.9	0.70	19.9	6.55	0.16	2.19	8.37	3.69	1.14	0.20	0	4	26	134	751	21	455	88	27	2.0	18	75	74	1	15	27	0	020205-2	G	26590/29757	Pre-1835 scoria fall	
4	57.2	0.71	19.7	7.03	0.17	2.09	8.15	3.59	1.19	0.20	4	4	22	126	787	24	459	97	27	1.3	19	97	83	4	11	28	3	030211-4	H	27657/33673	Pre-1835 scoria fall	
5	57.4	0.90	17.1	9.23	0.19	2.92	7.43	3.20	1.36	0.23	2	2	30	237	891	28	417	107	28	2.3	18	188	94	4	9	27	3	030211-1	320 m WSW of H	27346/33493	Old gray pumice of Tigüilotada	
6	57.4	0.74	19.1	7.09	0.16	2.28	8.10	3.67	1.22	0.20	3	4	23	147	778	24	447	96	28	1.9	20	66	86	4	9	17	3	030129-8	Between K & L	35022/40814	Brown scoria in 1835 fall	
7	57.5	0.74	18.9	6.90	0.17	2.22	8.08	3.83	1.23	0.20	1	1	25	125	812	23	437	94	29	2.0	18	94	81	3	6	20	0	020206-3	Between I & J	33542/38658	Dark gray scoria in 1835 pyroclastic flow	
COS5	57.5	0.70	18.9	7.08	0.15	2.31	8.04	3.67	1.16	0.21	5	14	23	162	783	22	454	91												Upper east flank		Scoria in 1835 fall; Set 2
8	57.6	0.73	18.9	7.28	0.16	2.23	7.92	3.73	1.25	0.20	5	4	23	139	797	25	440	98	28	1.1	20	98	86	4	6	25	3	030212-3	E	43085/26350	Scoria in 1835 pyroclastic flow	
9	58.0	0.73	18.8	7.20	0.17	2.20	7.71	3.74	1.29	0.21	4	4	23	135	814	26	437	99	29	1.6	20	97	83	7	7	26	1	030131-1	South rim	38489/33582	Caldera rim agglutinate of 1835	
COS9A	58.4	0.70	18.4	7.07	0.16	2.18	7.54	3.85	1.26	0.22	8	15	23	153	857	23	432	88												Upper east flank		Dense scoria in 1835 Set 3
COS3	58.4	0.71	18.3	7.09	0.16	2.16	7.49	3.78	1.29	0.28	7	18	23	144	825	23	434	97												East or south rim		Caldera rim agglutinate of 1835
10	58.5	0.76	18.4	6.88	0.17	2.20	7.50	3.88	1.32	0.22	2	5	27	136	855	26	422	100	31	1.5	19	67	84	2	16	16	1	020206-1	700 m east of L	36068/41307	Gray scoria of 1835 pyroclastic flow	
11	58.5	0.75	18.4	7.06	0.17	2.19	7.47	3.87	1.35	0.22	3	4	23	132	843	27	430	106	30	1.7	18	98	86	4	9	29	3	030201-1	2.5 km NNW of E	41804/28923	Dense juvenile lithic in 1835 fall	
12	59.1	0.76	18.0	6.77	0.17	2.21	7.17	4.04	1.36	0.22	1	5	28	115	876	27	406	103	31	1.7	18	80	85	5	22	24	4	020204-6	M	40297/40139	Black scoria in 1835 fall	
13	59.1	0.75	18.0	7.12	0.17	2.14	7.07	4.03	1.43	0.22	3	7	23	125	896	28	413	109	31	1.6	19	87	87	5	7	26	2	030129-1	L	35472/41663	Scoria in 1835 pyroclastic flow	
W	59.4	0.70	18.0	7.37	0.23	2.32	6.86	3.90	1.19	0.05																				North flank?		Scoria in 1835 pyroclastic flow
14	59.7	0.76	17.7	7.17	0.17	2.07	6.73	4.00	1.49	0.23	3	4	22	119	922	29	402	113	32	1.3	17	78	94	6	12	23	2	030129-7	Between K & L	35022/40814	Black scoria in 1835 fall	
15	59.8	0.77	17.6	6.81	0.17	2.12	6.71	4.17	1.46	0.23	1	2	21	110	922	29	395	109	32	2.5	19	74	85	0	18	19	2	020204-7	M	40297/40139	Brown scoria in 1835 fall	
16	63.8	0.71	15.7	6.32	0.17	1.49	4.42	5.06	2.06	0.26	5	7	19	51	1192	42	330	148	41	2.7	18	59	85	7	9	32	2	030129-4	L	35346/41305	White pumice in 1835 fall	
17	64.7	0.72	15.6	6.00	0.17	1.39	4.27	4.58	2.07	0.27	2	0	23	39	1256	43	314	148	40	3.3	16	48	92	6	3	39	2	020204-8	M	40297/40139	White pumice in 1835 fall	
18	64.8	0.76	15.3	6.83	0.18	1.40	4.49	3.77	2.23	0.24	4	8	21	65	1344	46	347	155	37	2.4	18	88	100	7	17	41	2	030211-2	320 m WSW of H	27346/33493	Old white pumice of Tigüilotada	



Figure 1

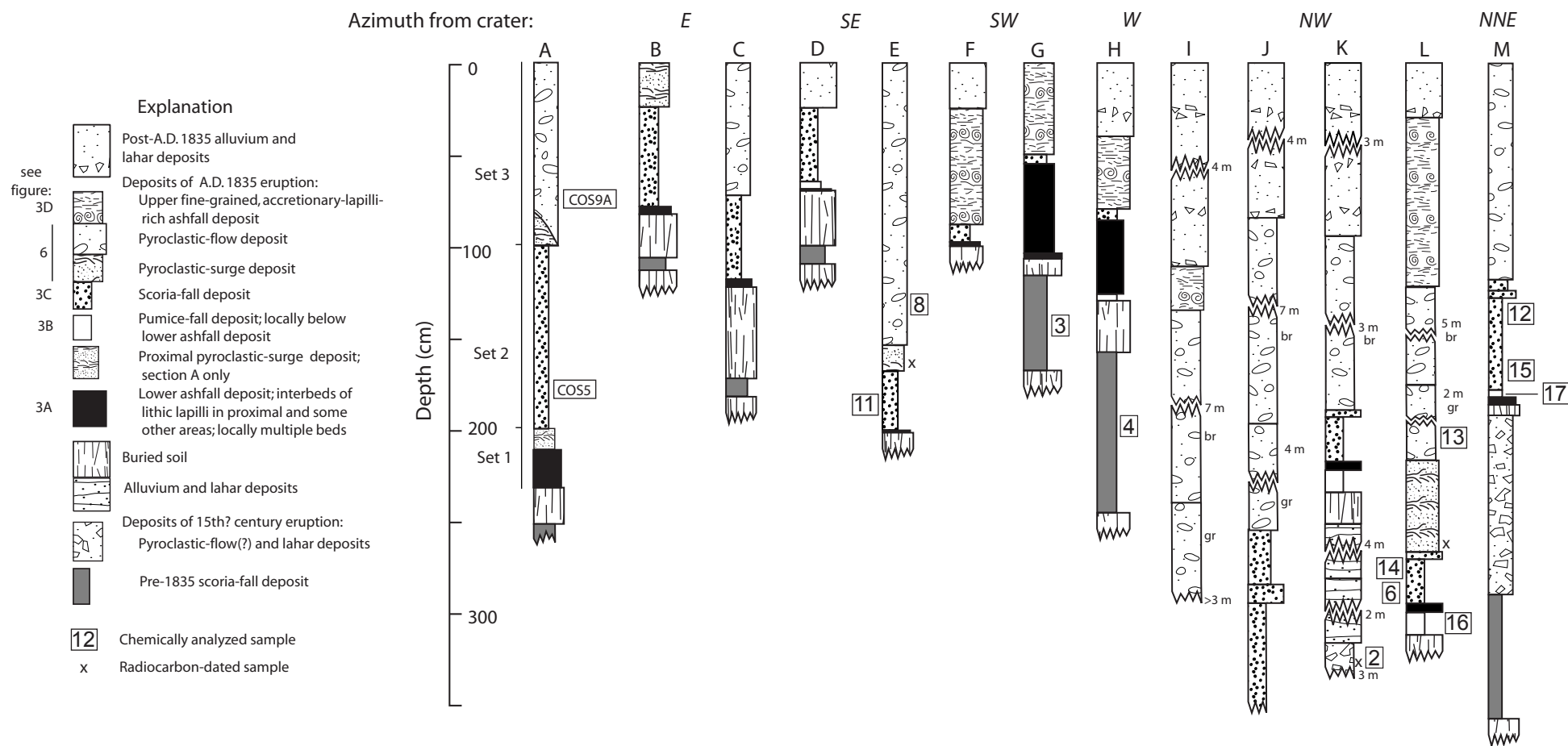


Figure 2

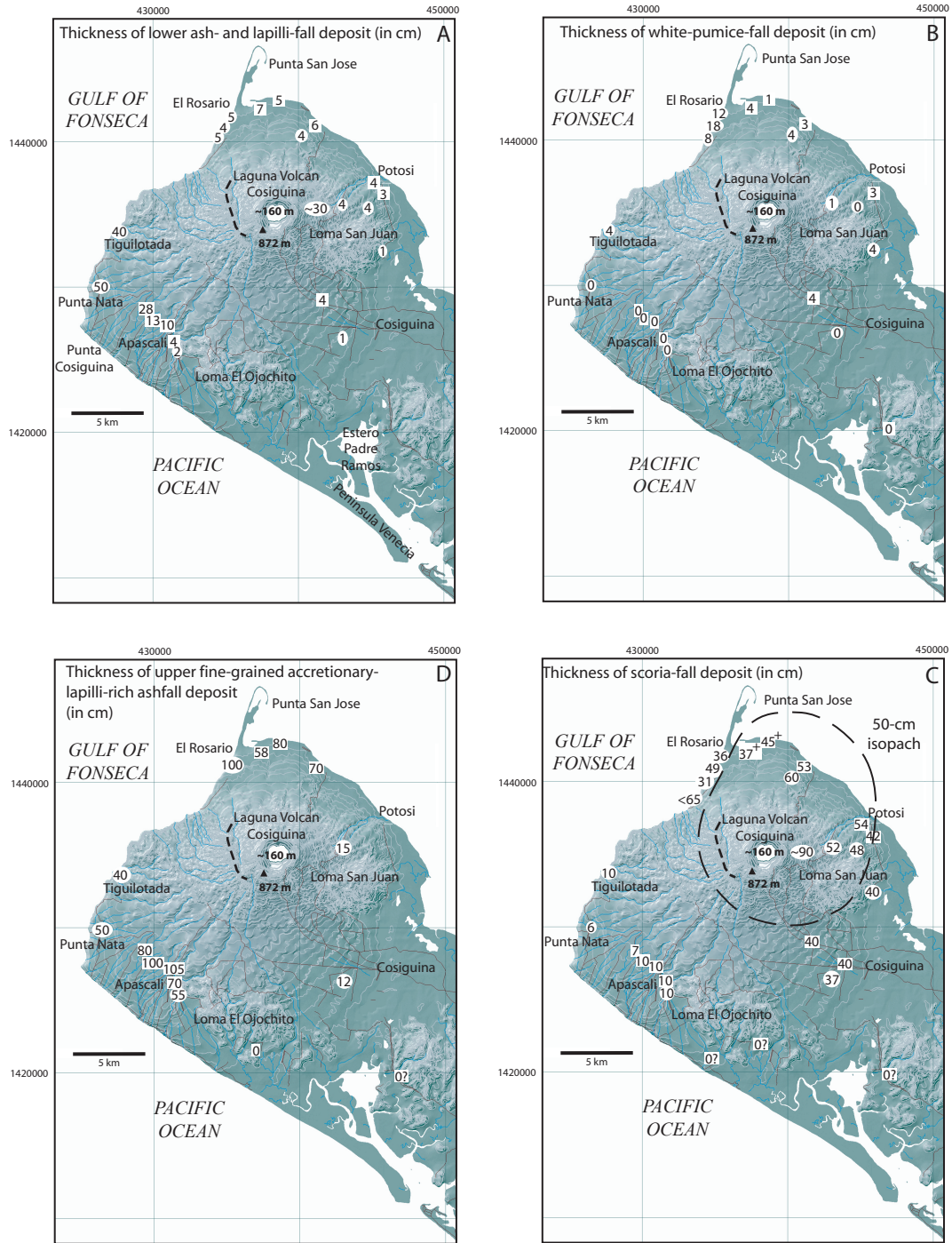


Figure 3

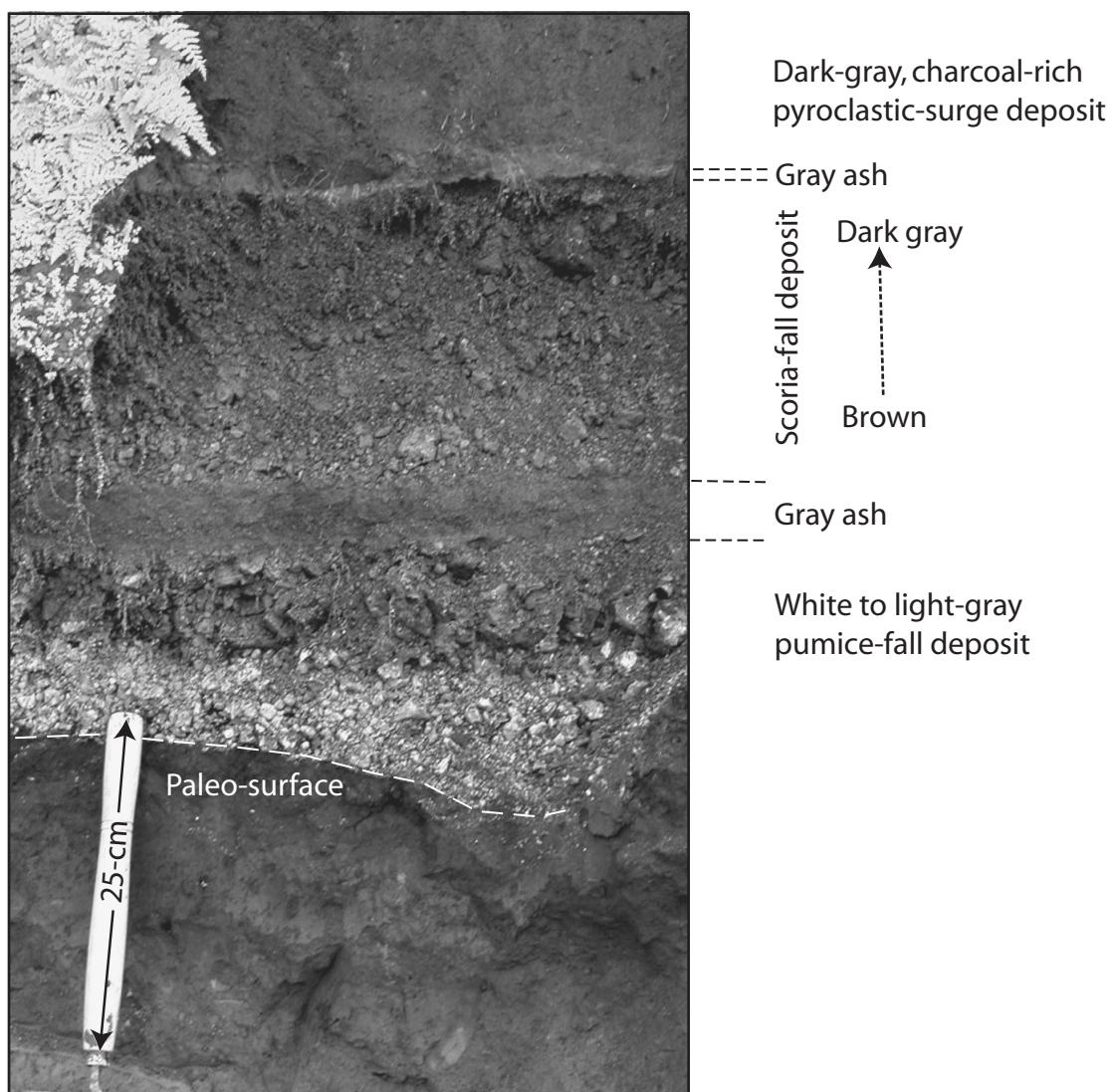


Figure 4

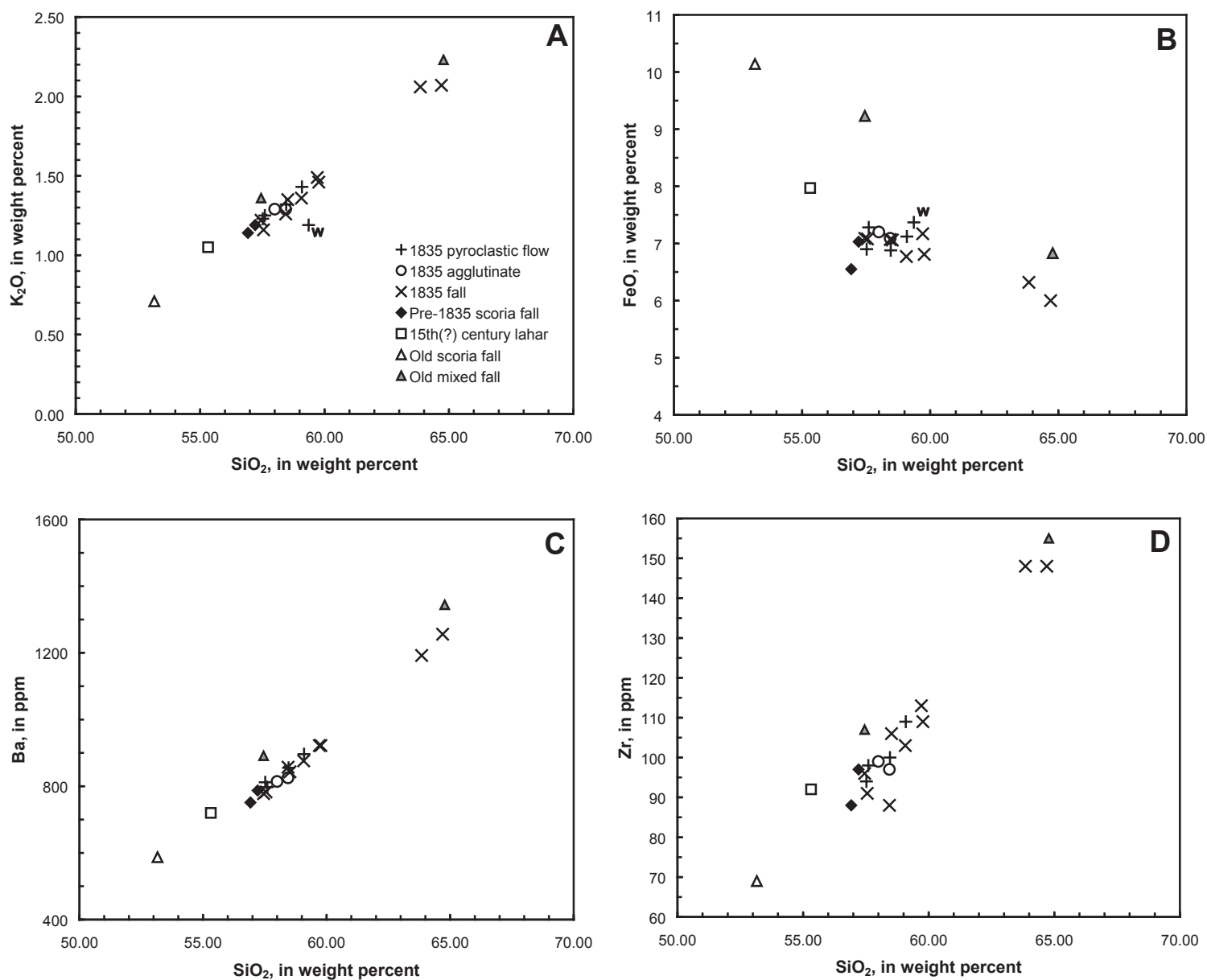


Figure 5

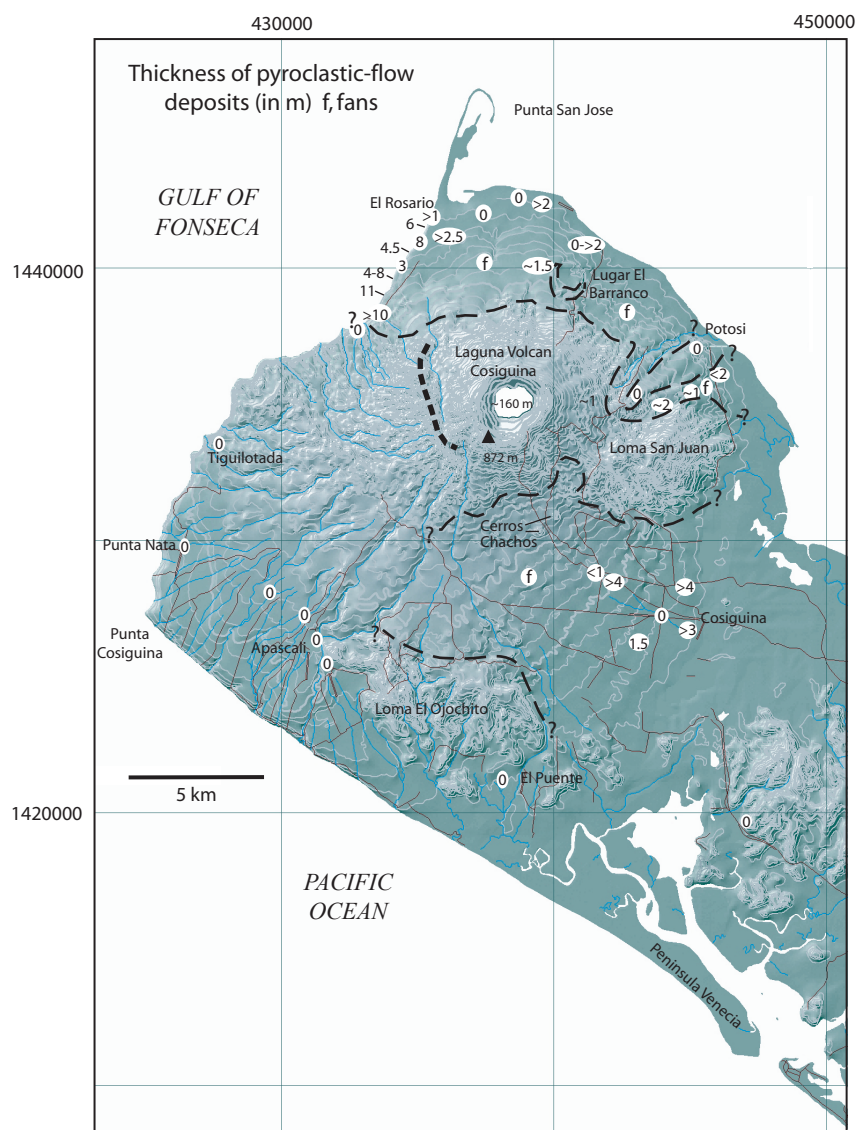


Figure 6

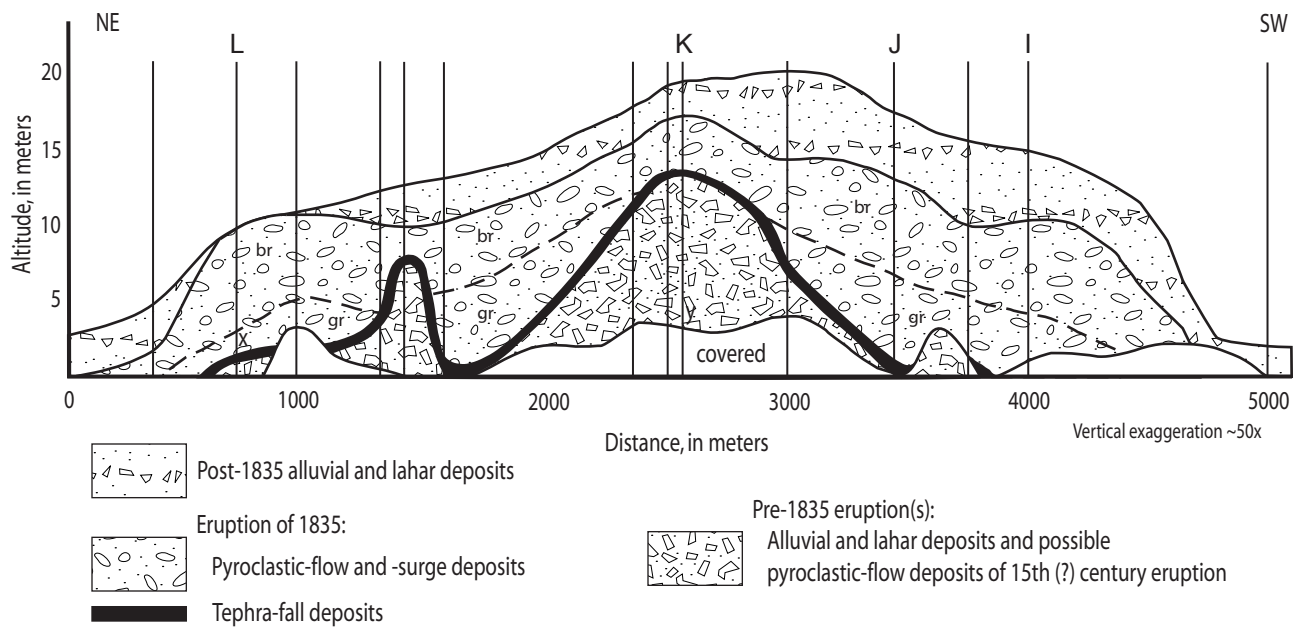


Figure 7

1-29-03-4
40814/35022
bwDSCN0681-pf-fa

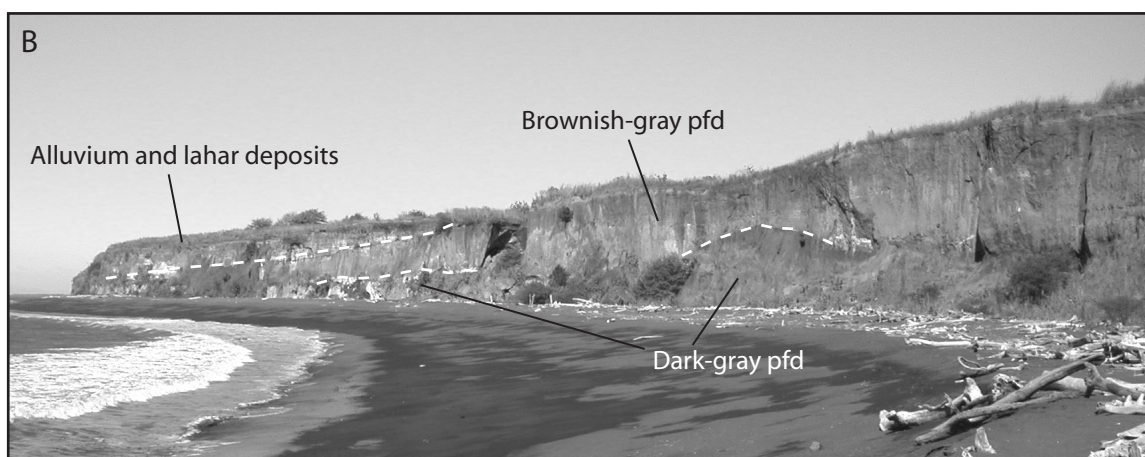
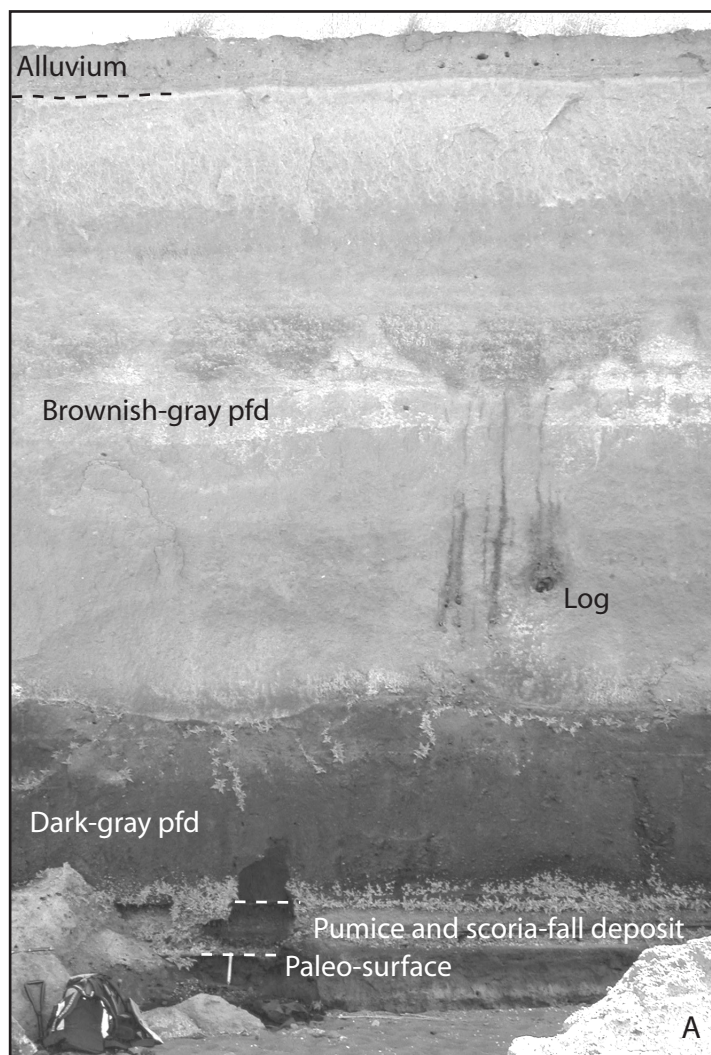


Figure 8

1-29-03-4
40814/35022
bwDSCN0681-pf-fa

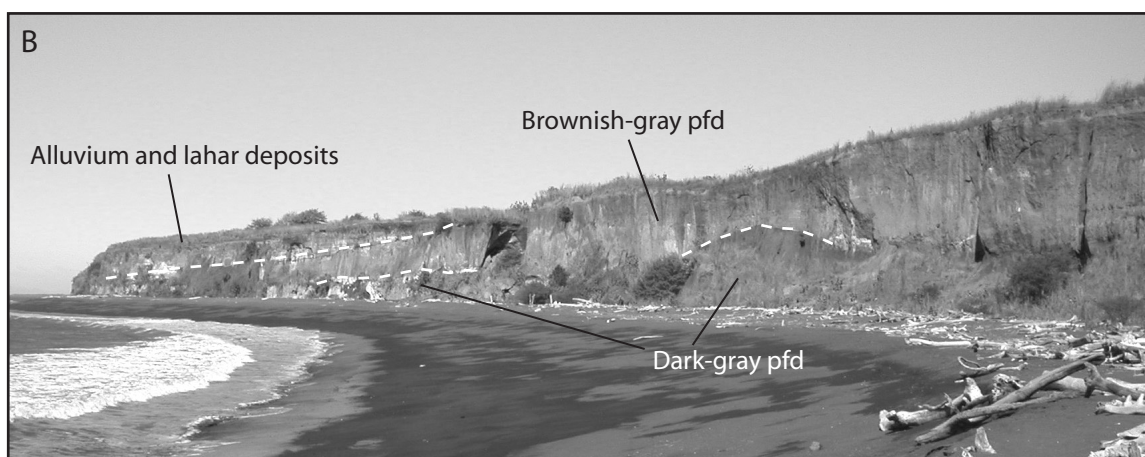
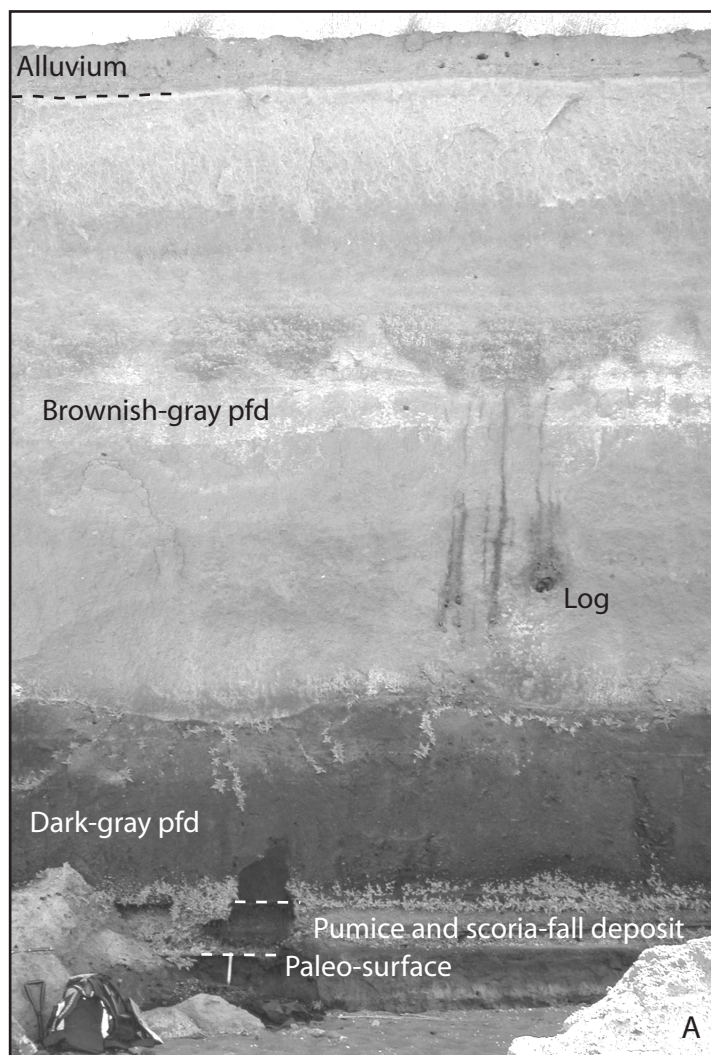


Figure 8

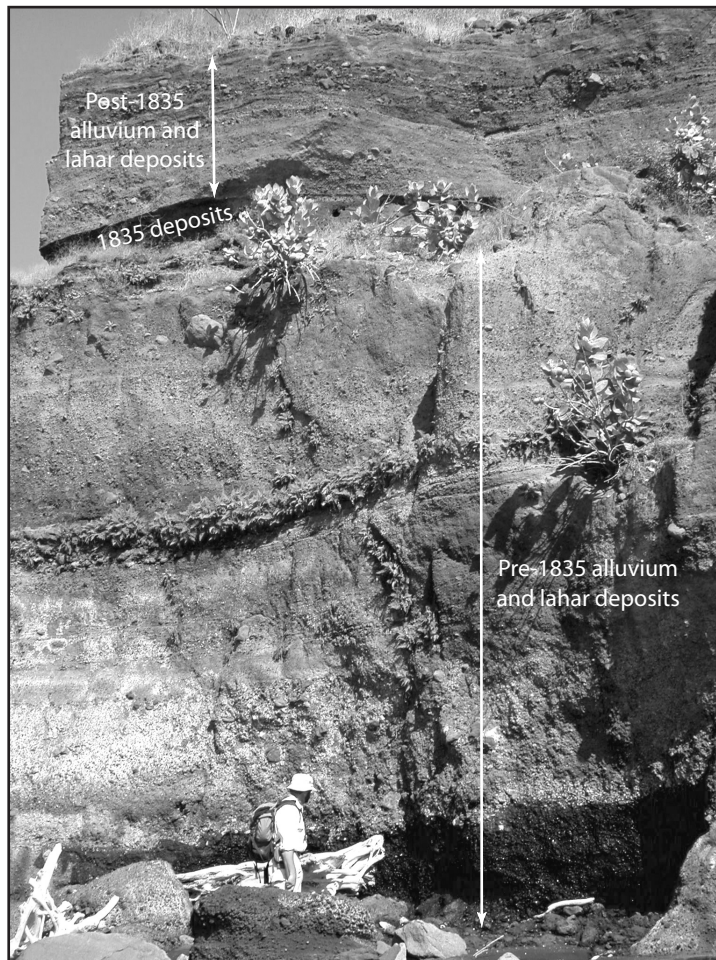


Figure 10



Figure 11

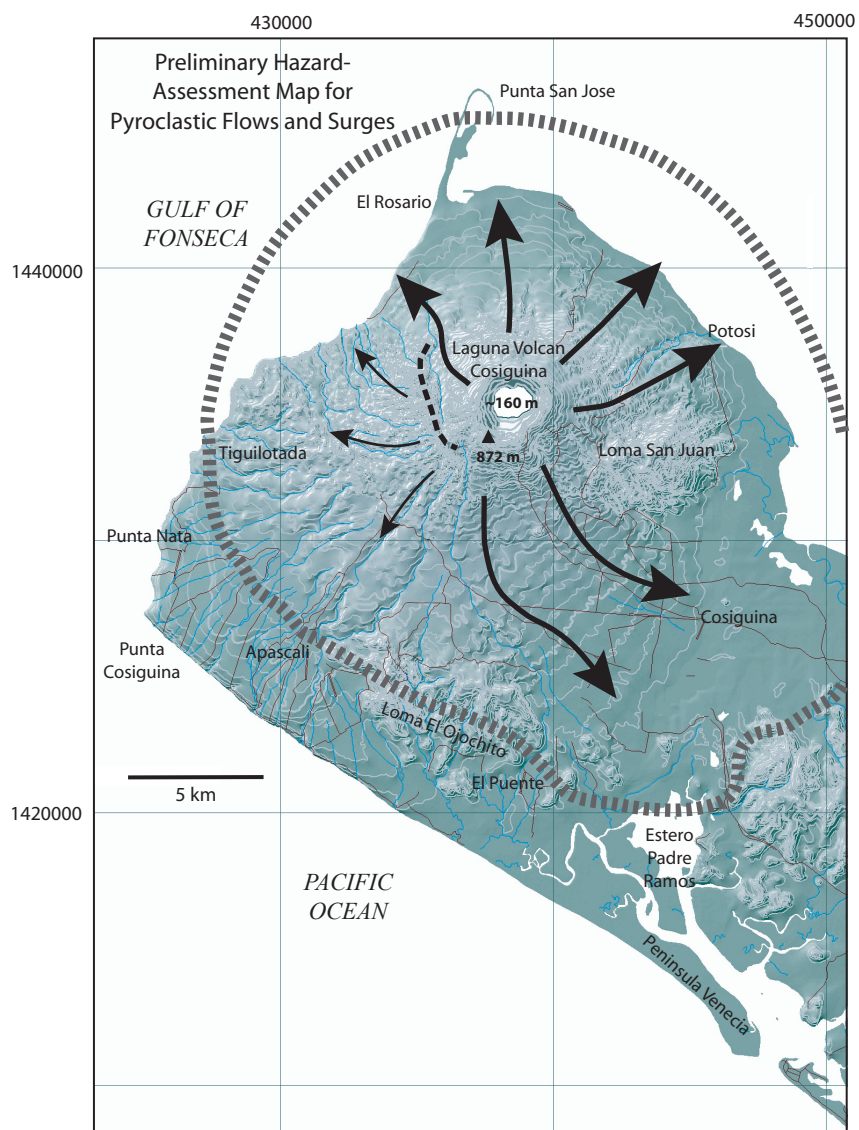


Figure 12

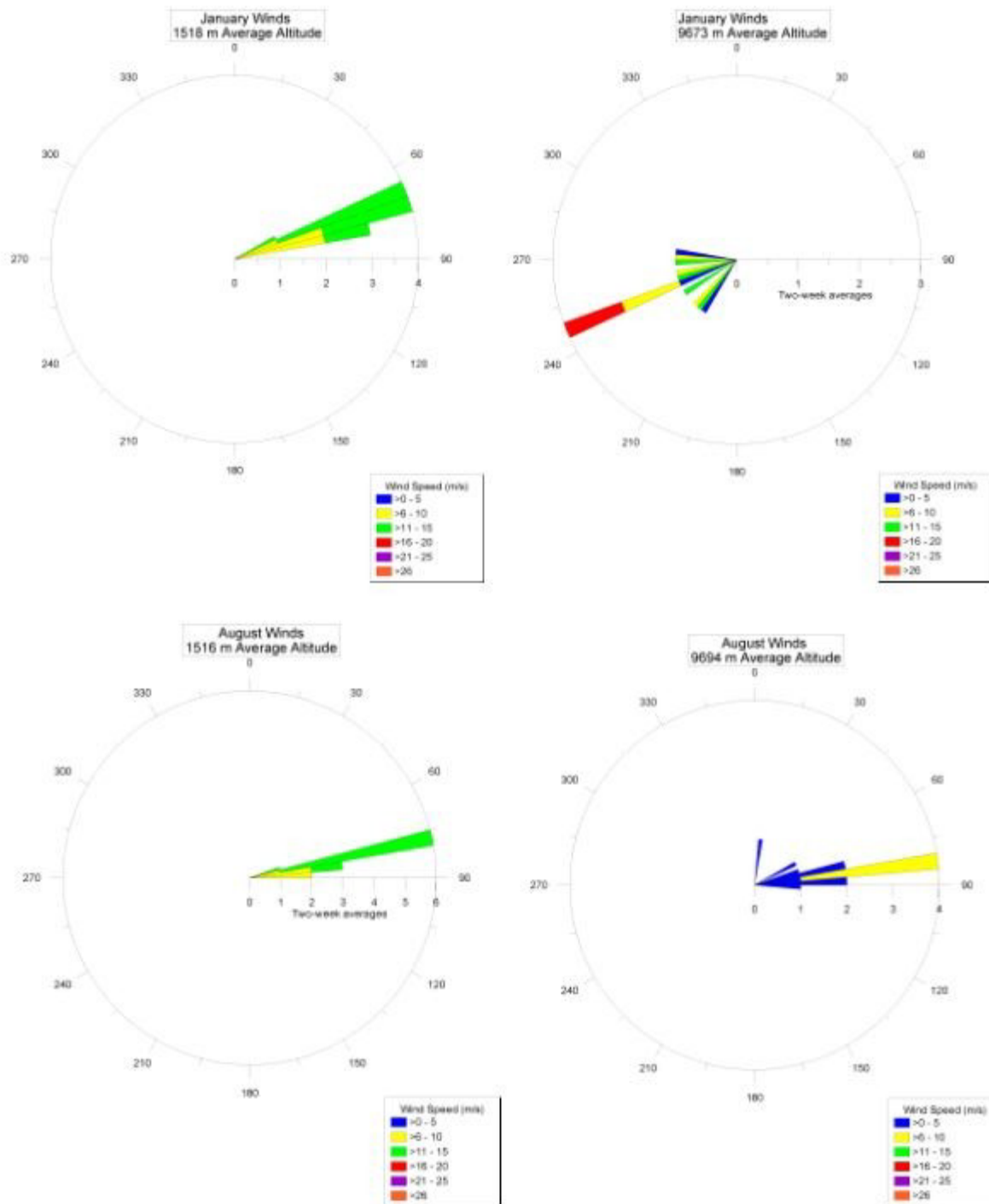


Figure 13 (to be replaced by black and white histograms)